Graphical Abstract

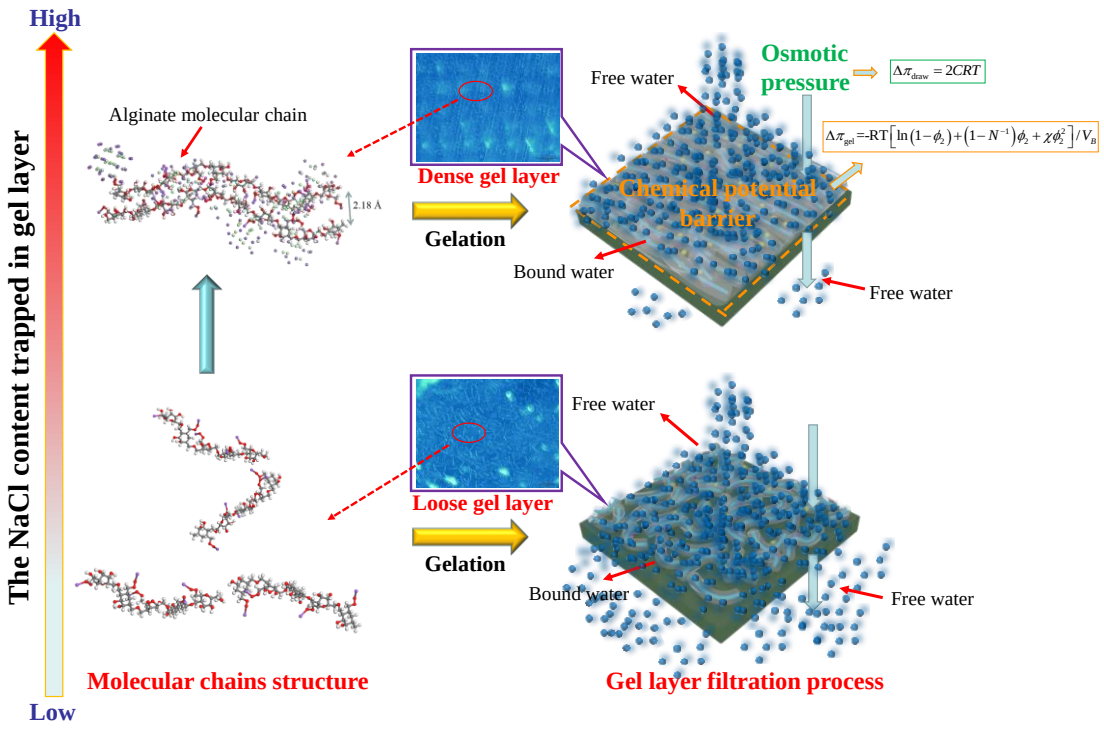

Novel molecular level insights into forward osmosis membrane fouling affected by reverse diffusion of draw solutions based on thermodynamic mechanisms

Jiaheng Teng [a], Hanmin Zhang [a*], Chuyang Tang [b], Hongjun Lin [c]

[a] Key Laboratory of Industrial Ecology and Environmental Engineering (Ministry of Education, MOE), School of Environmental Science and Technology, Dalian University of Technology, Linggong Road 2, Dalian, 116024, China

[b] Department of Civil Engineering, The University of Hong Kong, Pokfulam, Hong Kong, 999077, China

[c] College of Geography and Environmental Sciences, Zhejiang Normal University, Jinhua, 321004, China

[*]Corresponding author. zhhanmin@126.com

Abstract

Forward osmosis membrane bioreactor (FOMBR) has a more intricate membrane fouling mechanism than MBR because of the special existence of the reverse diffusion of draw solution. The mechanisms of membrane fouling affected by reverse diffusion of draw solution and ion content in gel layer were investigated from thermodynamic perspective and molecular level in this study. Phase-contrast microscopy non-invasively observed that the molecular chain structure of the gel layer containing low content of reverse diffused solute (NaCl) was sparse, while the alginate molecular chains with high NaCl content were parallel and compact. Density functional theory (DFT) further simulated the formation mechanism of different alginate chain structures, that is, the reverse diffused solute shortened the distance between hydrogen bonds and reduced the interaction energy at the terminals of alginate chains. This proved that the NaCl trapped in alginate layer directly affected its structure. Heating experiments indicated that gel layer acted as a "chemical potential barrier" that prevented bound water from turning into free water. Accordingly, the "chemical potential barrier" described by Flory-Huggins theory was proposed, which was confirmed to account for the filtration of alginate gels affected by reverse diffusion of draw solution. To the best of our knowledge, this is the first membrane fouling study that explores the effect of reverse diffusion of draw solution on the "chemical potential barrier" of gel layer from perspective of molecular chain structure. This study investigated FOMBR fouling mechanism at molecular level and provided a new strategy for FOMBR system fouling quantification.

Keywords

FOMBR membrane fouling; reverse diffusion of draw solution; molecular chains observation; chemical potential barrier; density functional theory

1. Introduction

Stringent regulations and global water shortages place a great demand for efficient water treatment technologies [1-3]. For dealing to these intractable challenges, developing an efficient membrane bioreactor (MBR) technology is a realistic option [4]. FOMBR is viewed as a promising alternative of MBR since it demonstrates better removal efficiency and requires no external pressure [5-7]. Unfortunately, both MBR and FOMBR are subjected to membrane fouling, which increases the cleaning frequency and shortens the membrane life span [8-10]. What is different between FOMBR fouling and MBR fouling is that reverse diffusion of draw solute exerts a seriously adverse impact on the fouling behavior and property of fouling layer [11-13]. Up to now, most of efforts have been focused to study the flux decline behavior, while limited attention has been paid to the effects of reverse diffusion of draw solution on the formation thermodynamic process and properties of fouling layer [11, 14]. Therefore, there is an imperative requirement for in-depth understanding of FOMBR fouling, especially the thermodynamic mechanisms of membrane fouling affected by reverse diffusion of draw solution [15].

Gel layer is generally considered as the principal cause to MBR fouling, and its specific filtration resistance (usually at level of 10^{16}-10^{17} $m \cdot kg^{-1}$) can be a few orders of magnitude higher than that of cake layer even though the former has much thinner thickness [16-19]. In MBR, the formation of gel layer is a spontaneous process from the thermodynamic viewpoint because the macromolecular foulants (soluble microbial products (SMP) and extracellular polymeric substances (EPS)) tend to adsorb/mix as much water as possible to form a stable swelling gel layer [20-24]. Recent studies have shown that the gel layer formed by this process is non-porous, impervious and homogeneous. Thus, filtration through a gel layer is considered

to drag the bound water from gel layer to become free water in the permeate. It is required to overcome water chemical potential gap ($\Delta\mu$) between permeate (high water chemical potential) and gel layer (low water chemical potential) when dragging bound water from gel layer to the permeate during filtration process [21, 25-27]. The osmotic pressure gap ($\Delta\pi$) on both sides of FO membrane provides a driving force to overcome this water chemical potential gap ($\Delta\mu$). While gel layer is equivalent to a "chemical potential barrier" which offsets a part of driving force, resulting in a great decrease in filtration efficiency [17, 25]. Moreover, the reverse diffused solute is partially trapped in gel layer. As a result, the ion content of gel layer in FOMBR is much higher than that in MBR, leading to significant changes in the formation process and properties of gel layer [28]. Singh et al. suggested that the interaction of gels with ion increased the viscosity of gel layers [29]. Derjaguin-Landau-Verwey-Overbeek (DLVO) theory has pointed out that the high ionic strength compresses the electric double layer and weakens the electrostatic repulsion force between gel molecules, thereby contributing to the formation of a dense gel layer [30-32]. FOMBR fouling involves a complex interaction between reverse diffused solute and foulants, which is far more complicated than pressure-driven MBR fouling. Therefore, further research on the interaction mechanism of the binary complex system composed of reverse diffused solute and foulants is of great significance to improving our insights into FOMBR fouling [5, 33].

The purpose of this study is to explore the underlying mechanism of FO membrane fouling affected by reverse diffusion of draw solution. Phase-contrast microscopy was used to observe the original molecular chain structure in fresh gel layer formed in draw solutions with different ionic strength. The molecular chain structure of gel layer with different content of reverse diffused solute were accurately predicted by the classical quantum mechanics method called

DFT. The simulation results might help further explain formation mechanisms of different molecular chain structures of gel layer. Finally, the membrane fouling of gel layer affected by reverse diffusion of draw solution was elucidated by combining molecular chain structure of gel layer with Flory-Huggins lattice theory from the perspective of water chemical potential. This research will not only provide insights into FO membrane fouling mechanism but also blaze a new way in the investigation into membrane fouling.

2. Materials and methods

2.1. Samples preparation

It is generally accepted that fouling layer is a mixture of many compounds, and the fouling behavior of real fouling layer could be satisfactorily simulated by a model foulant when studying the mechanism of membrane fouling [27, 34-36]. In previous studies, sodium alginate (SA) is frequently used as a model compound for gel layer in membrane fouling study due to its availability and high ability to form a gel layer, and sludge floc suspensions were most commonly used to form a cake layer [20, 37-39]. The alginate solutions (1.0 g/L) were prepared by dissolving 2.0 g SA powder into 2000 mL deionized (DI) water with continuous magnetic stirring for 2 h until the SA powder completely dispersed. The sludge floc suspensions (1.0 g/L) were obtained by centrifuging the active sludge at 5000 g for 5 min and sediment was diluted with a buffer solution (2 mM K_3PO_4, 4 mM KH_2PO_4 and 10 mM KCl) at pH 7 [38]. The active sludge obtained at stable operation stage of a lab-scale FOMBR. The alginate solutions and the sludge floc suspensions samples were used for fouling tests.

2.2. Batch fouling tests

Batch FO fouling tests were conducted to compare the fouling behavior between model gel

foulants (alginate solutions) and sludge floc suspensions affected by reverse diffusion of draw solution. As shown in Fig. 1, an external FOMBR was used to explore the membrane fouling behaviors affected by reverse diffusion of draw solution in this paper. The membrane module is placed outside the bioreactor, and the model gel foulants and sludge floc suspensions flow through the FO membrane in a circulating manner. To study the effect of reverse diffusion of draw solution on FO membrane fouling, same volume (500mL) of foulants (prepared according to section 2.1) were filtered in draw solution with different ionic strength (1, 2, 3, 4 mol/L NaCl solutions). By plotting the relationship between flux and permeate volume instead of the flux versus time [40]. Moreover, to eliminate the continuous dilution of draw solution caused by the penetration of water during the filtration process, baseline experiments were carried out before batch fouling tests.

The weight of permeate was recorded in real-time with a balance connected to a computer, and each fouling test was conducted 3 times. The working temperature maintained at about 25 ℃. According to literature, the membrane flux (J, L/(m^2·h), LMH) could be calculated by [41]:

$$J = \frac{\Delta V}{A_m \Delta t} \quad (1)$$

where ΔV is the permeate volume (L), Δt is the time interval (h), and A_m is the FO membrane effective area (m^2). The conductivity values of feed solution and draw solution were obtained at intervals of 60 s, and the conductivity value is then used to calculate ion concentration. The osmotic pressure (π) of the solution was calculated based on the empirical equation [42]:

$$\pi = 4.5032C^2 + 43.6426C \quad (2)$$

where C is the ion concentration (mol/L).

The osmotic pressure gap ($\Delta\pi_{drive}$) between draw solution and feed solution provides a driving force for FO membrane filtration:

$$\Delta\pi_{drive}=\pi_{draw}-\pi_{feed} \quad (3)$$

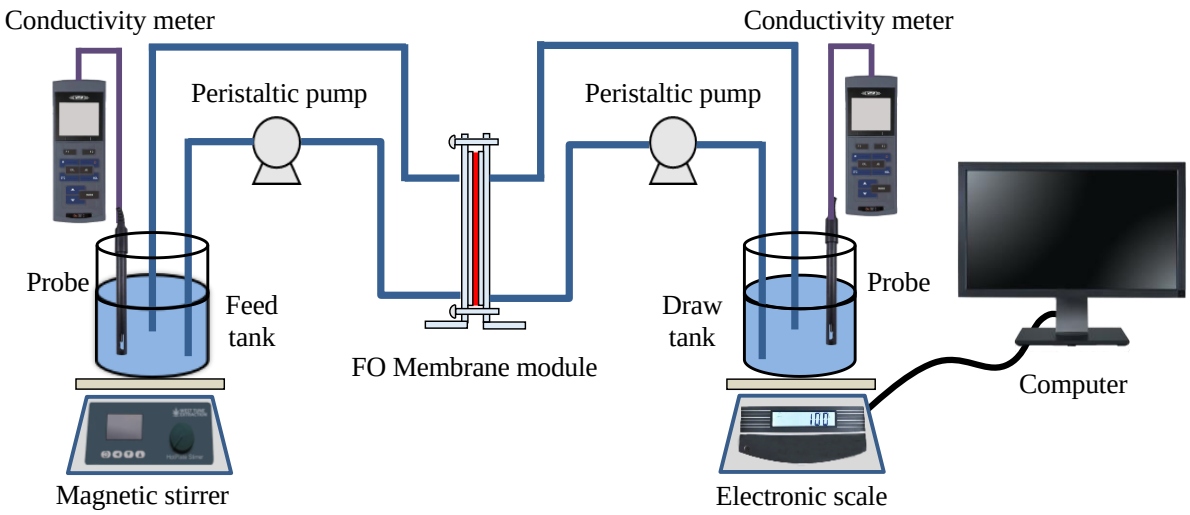

Fig.1. Schematic of the lab-scale external FOMBR.

2.3. Novel non-invasive microscopic observation method of gel layer microstructure

In this study, all alginate fouling layer samples used for subsequent experimental characterizations were formed by filtering 500 mL of foulants. Fresh gel layers are thin and transparent, and their microstructure cannot be directly observed by a conventional optical microscope [8]. Moreover, other observation methods such as SEM require freeze-drying the fouling layer for 24 hours and spray gold in vacuum before characterization. This process unavoidably destroy the original structure of gel layer, which necessitates the development of a novel method that can observe the microstructure of a transparent material without harming its original structure [43]. Phase-contrast microscope is a better alternative choice. It has been

extensively used to observe unstained cells owing to its capability of checking out the extremely fine structure in transparent materials through the diffraction and interference of light without damaging samples [44]. In this study, microscope images of fresh alginate gel layers were observed by an Olympus IX83 inverted microscope (Olympus America Inc., PA, USA) in phase (ph) mode.

2.4. Analytical methods

2.4.1. Chemical analyses

Fresh alginate layers were further dried in a vacuum freeze dryer (LC-10LCN, China) for 24h before their functional groups were characterized by Nicolet iN10 Fourier Transform Infrared Spectrometer (FTIR). The spectra in the range of 4000-500 cm^{-1} were collected by overhead and removable multi reflective attenuated total reflection accessory (ATR). The chemical composition of alginate layers was determined by an X-ray photoelectron spectrometer (XPS) (ESCALAB 250Xi, Thermo Fisher Scientific, USA) with Al-K X-ray as the excitation source.

2.4.2. Thermal stability of alginate gel layers

Thermal stability of alginate gel layers was measured by a thermogravimetric analyzer (Q200, TA Instruments, Germany). Fresh gel samples were placed in an Al_2O_3 crucible and heated to 600℃ at a heating rate of 10℃/min under the nitrogen atmosphere. Moreover, heating experiments were conducted to investigate the ability of gel layers to bind with water. Fresh gel layers were placed in a constant temperature oven (WRF-Q800, China) for 1 hour at 35℃, and their weight changes were recorded.

2.4.3. Inductively coupled plasma optical emission spectrometer (ICP) analysis

As the reverse diffused draw solute is trapped in gel layer, it is bound to produce a certain osmotic pressure. Gel layer samples were completely dissolved in deionized (DI) water by magnetically stirring for 2 hours. An inductively coupled plasma optical emission spectrometer (Nex ION 300D, PerkinElmer, USA) was utilized to detect the concentration of NaCl that was trapped in gel layers, followed by the calculation the osmotic pressure of the ions trapped in alginate gel layers according to Eq.2.

2.5. DFT calculations

Density functional theory (DFT) is a classical quantum mechanical method used to study the properties of molecules, which is one of the most commonly used methods on computational chemistry [45, 46]. The DFT computational of molecular structure and binding energy can provide accurate prediction for the interaction between reverse diffused solute (NaCl) and sodium alginate chains. Quantum chemical calculations were performed with the Gaussian 09 program by using DFT/B3LYP hybrid method. In this study, a short alginate chain model containing 10 uronic units and a long alginate chain model containing 20 uronic units were established, and each alginate chain contained six uronic rings [47]. The 6-31 G basic set was used to optimize the molecular geometry and yield energy data. Based on quantum chemistry calculation results, the effect of reverse diffusion of draw solution on the interactions between alginate chains was explored at the molecular level.

2.6. Flory-Huggins lattice theory

The lattice theory proposed by Paul Flory and Maurice Huggins is a mathematical model that describes the thermodynamics of polymer solutions [48, 49]. In previous studies,

Flory-Huggins lattice theory was proposed to describe the water chemical potential change in the formation process of gel layer [47, 50]. According to Flory-Huggins theory, the change in Gibbs free energy during filtration can be described by [48, 51]:

$$\Delta G = RT\left[\mathrm{n}_1 \ln \phi_1 + \mathrm{n}_2 \ln \phi_2 + \mathrm{n}_1 \phi_2 \chi\right] \quad (4)$$

where n and ϕ represent mole number and volume fraction, respectively; the subscripts of 1 and 2 mean solvent and solute, respectively; χ is the Flory-Huggins interaction parameter. As $\phi_1 + \phi_2 = 1$, the chemical potential change ($\Delta\mu$) of this process is given as follows:

$$\Delta\mu = RT\left[\ln\left(1-\phi_2\right) + \left(1-N^{-1}\right)\phi_2 + \chi\phi_2^2\right] \quad (5)$$

where N is the degree of polymerization of cross-linked polymer, which is usually assumed to infinity.

3. Results and discussion

3.1. Effects of reverse diffusion of draw solution on filtration behavior

Fig. 2 shows the effects of reverse diffusion of draw solutions with different ionic strength (1M, 2M, 3M, 4M NaCl solutions) on the filtration behavior of different feed solution (DI water, sludge floc suspensions, and alginate solutions). In this study, same volume and same mass concentration of foulants (500mL, 1.0 g/L) were filtered in each filtration tests, which therefore the draw solution was diluted to same degree. As indicated by Fig. 2, the DI water flux decline ratio approximated to 9.0% for all cases (8.3%, 9.0%, 8.5% and 9.5%, respectively), which was mainly ascribed to dilution of draw solution [52]. As for sludge floc suspensions, the water flux decline ratio was near 30% under all the circumstances (27.8%, 29.8%, 27.5% and 29.9%, respectively), suggesting that the membrane fouling caused by sludge floc suspensions are

moderate. Obviously, the reverse diffusion of draw solution has negligible effects on the filtration behaviors of DI water and sludge floc suspensions. In contrast, the flux decline ratio of alginate solutions increased dramatically (17.2%, 28.8%, 56.9% and 69.2%, respectively) with the increase of the ionic strength of draw solutions. Thus, it is considered that that the filtration behavior of alginate solutions was considerably affected by reverse diffusion of draw solution, and extremely severe alginate fouling occurred at draw solutions with high ionic strength.

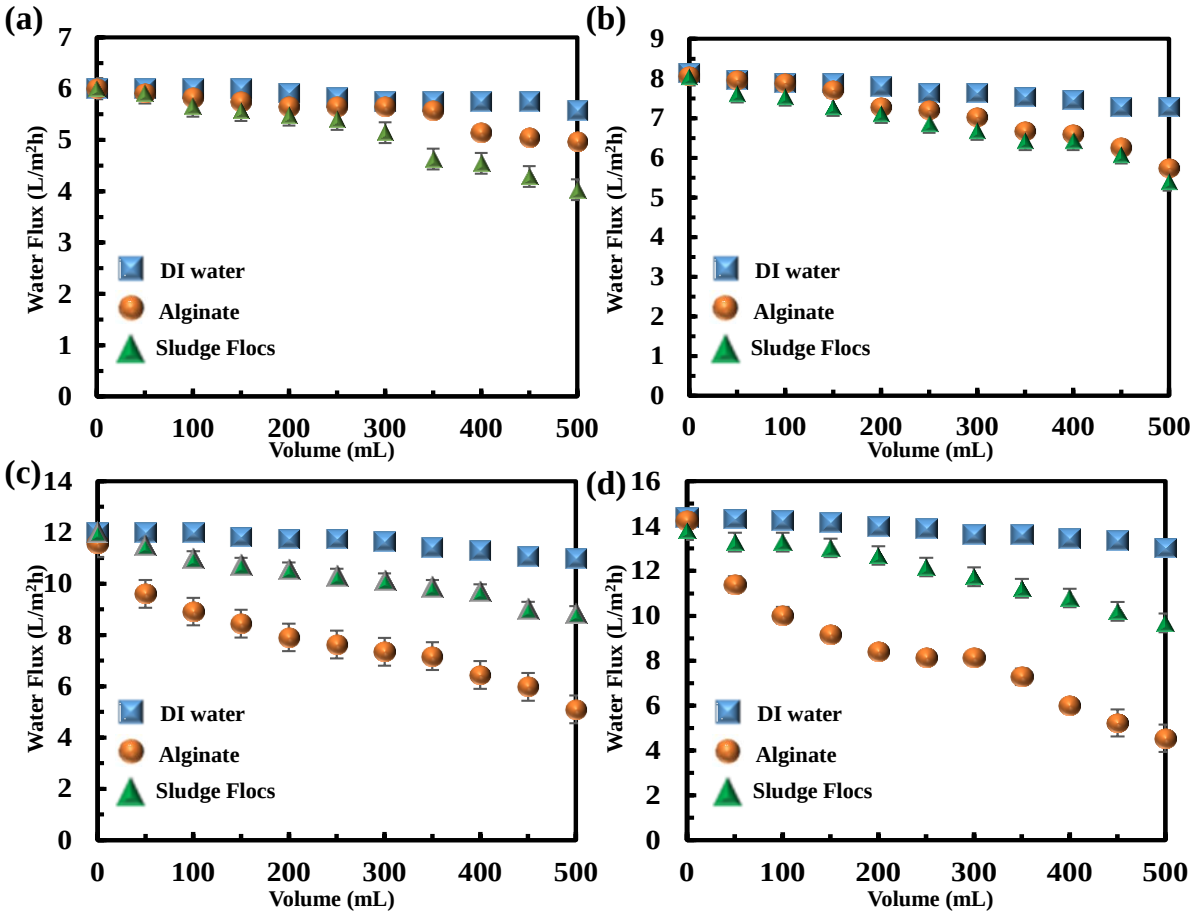

Fig. 2. Effects of reverse diffusion of draw solutions with different ionic strength ((a) 1 M, (b) 2 M, (c) 3 M and (d) 4 M NaCl solutions) on the filtration behavior of DI water, sludge floc suspensions and alginate solutions.

Fig. 3 shows the optical images of fouling layers formed on FO membrane surface in draw solutions with different ionic strength, the appearance of these layers is completely different. It

can be seen from Fig. 3(a1)-(a4) that the cake layers formed by sludge floc suspensions are loose and powdery. The weights of cake layers are 0.316±0.015g, 0.293±0.025 g, 0.299±0.023 g, and 0.306±0.011 g, respectively, which are not significantly different. Contrary to sludge floc suspensions, the alginate retained on FO membrane surface shows typical gelling properties (Fig. 3(b1)-(b4)). The weights of gel layers gradually increase (0.237±0.013 g, 0.666±0.020 g, 1.139±0.170 g, and 1.518±0.110 g, respectively) with the rising concentration of draw solutions. It should be noted that the filtration experiments were performed under the conditions of same volume (500mL) and same mass concentration (1.0 g/L) of foulants. Thus, it is considered that the reverse diffusion of draw solution significantly affects the FO membrane fouling behavior of alginate gel foulants, which directly causes severe FO membrane fouling. Overall, the main effect of reverse diffusion of draw solution on FO membrane fouling is that its significant impacts on gel layer fouling rather than cake layer fouling.

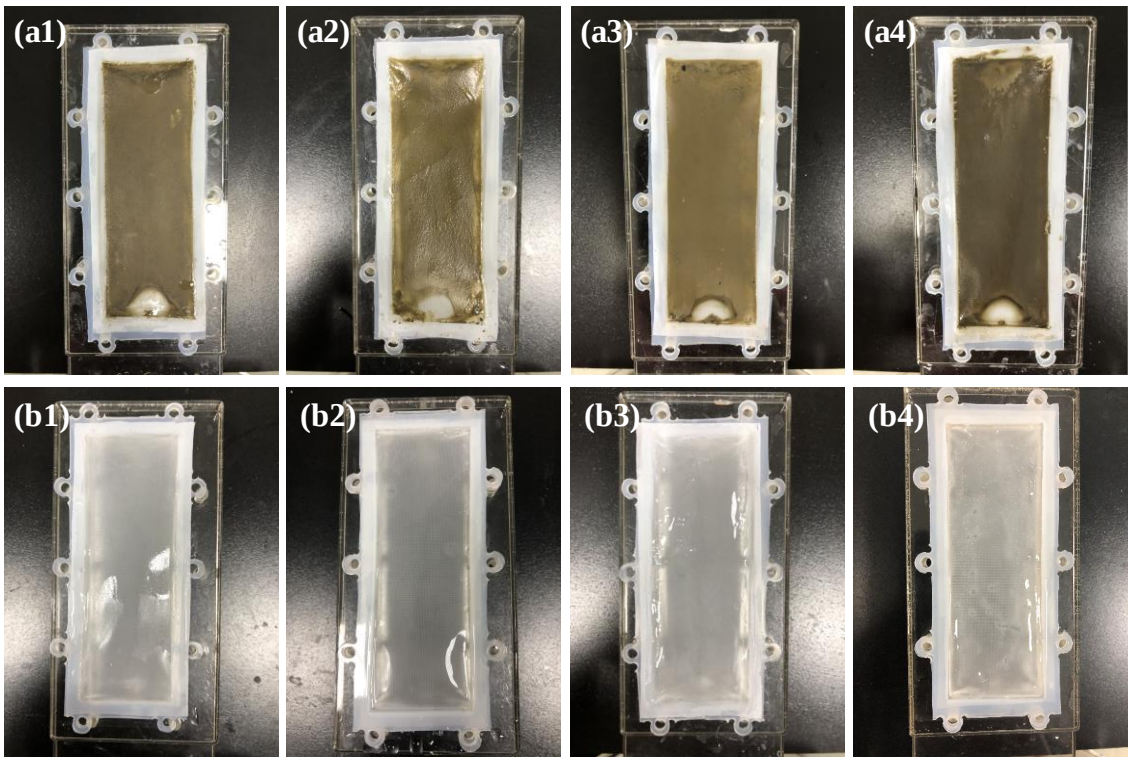

Fig. 3. Optical images of foulant layers in draw solutions with different ionic strength. (a)

Sludge flocs layer, and (b) alginate layer. 1, 2, 3, and 4 refer to 1M, 2M, 3M, and 4M NaCl solutions, respectively.

Fig. 4 shows the content of NaCl trapped in different SA layers formed by same volume of SA solutions filtered through draw solutions with different ionic strength. The content of NaCl trapped in SA gel layers increased almost linearly from 0.0690±0.01283 mol/L to 0.6090±0.01778 mol/L, indicating that reverse diffusion of draw solution directly affected the NaCl content in gel layers. Due to the inevitable reverse diffusion of draw solution during FO process, the ion content in FOMBR gel layer was much higher than that in MBR gel layer. A recent study showed that, adding a small amount of NaCl (0-250mM) to the alginate solution significantly changed the fouling layer from a sparse structure to a dense structure and greatly improved the filtration resistance, which indicated that NaCl played a vital role in the structure change of the alginate fouling layer [28]. Thus, the critical effects of ion content in gel layers on FOMBR fouling behavior should be highlighted [28, 53, 54].

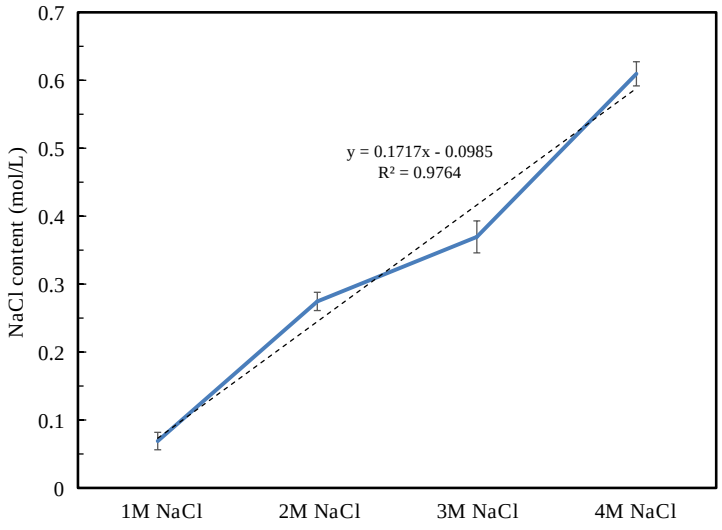

Fig. 4. The content of NaCl trapped in different SA layers due to the reverse diffusion of draw solutions with different ionic strength.

3.2. Characterizations of alginate layers formed in draw solutions with different ionic strength

3.2.1. Functional groups analyses

Fig. 5 represents the ATI-FTIR spectra of alginate gel layers formed in three draw solutions with different ionic strength. Five typical alginate characteristic peaks and the corresponding functional groups are ~3260 cm^{-1} (−OH), ~2930 cm^{-1} (−C−H), ~1602 cm^{-1} (>C=O), ~1408 cm^{-1} (−COO−) and ~1016 cm^{-1} (−C−O), respectively [55]. The FTIR spectra of all alginate layers are similar to each other, which probably suggests that the FTIR technique may not detect difference in the functional group compositions of these samples.

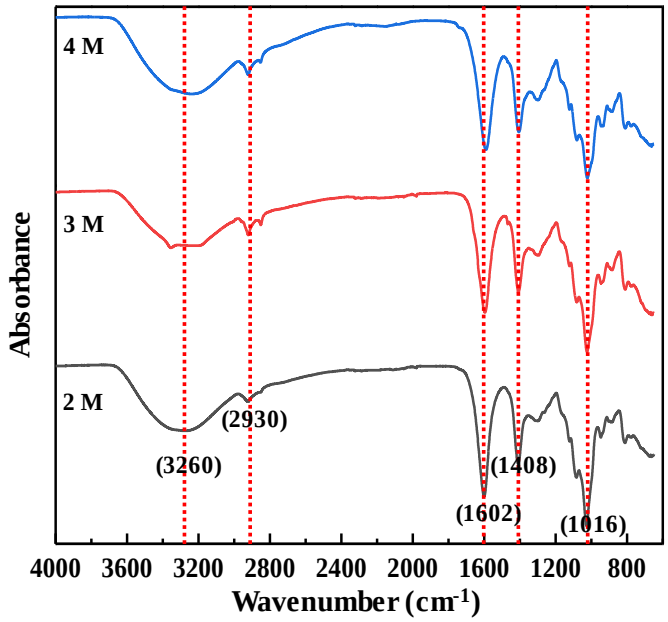

Fig. 5. FTIR spectra of alginate layers formed in draw solutions with different ionic strength.

Fig. 6 shows the XPS spectra of C1s and O1s of gel layers formed in draw solutions with different ionic strength. In Fig.6(a1)-(c1), C1s signals at 287.7, 286.2, 285.7, and 284.5 eV correspond to the O-C=O, O-C-O, C-O and C-C bonds, respectively [56]. The O1s signals at 532.6, 531.9, and 530.9 eV represent the -C=O-O, C-O and C=O bonds, respectively, as

indicated by Fig. 6(a2)-(c2). It can be seen that the proportion of groups only changed slightly, and the binding energy of the C and O chemical bonds of the alginate did not move. Some studies suspected that different fouling behaviors were caused by the difference in the functional groups of foulants [57]. These chemical characterization results clarified that the reverse diffusion of draw solution or the ion content in gel layers could not significantly affect the functional group of alginate gel layer. In other words, the tiny differences in functional groups may not be the underlying cause for the dramatically different fouling behavior (Figs. 2 and 3). Further research is required.

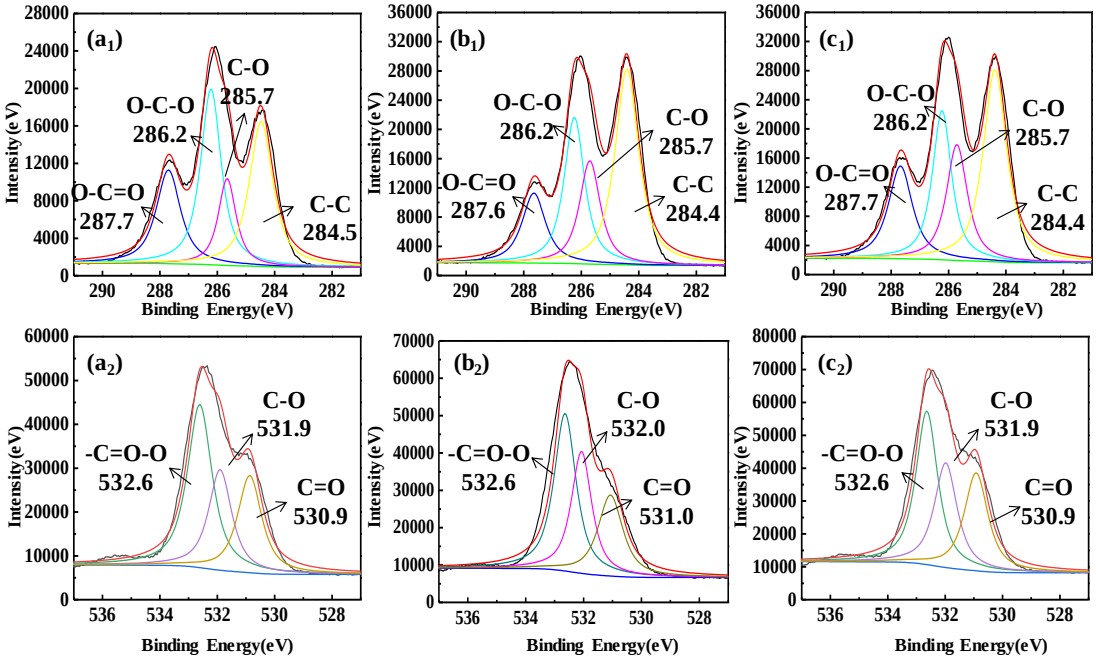

Fig. 6. XPS spectra of alginate layers formed in draw solutions with different ionic strength. (a) 2 M, (b) 3M and (c) 4 M NaCl solutions, and the post-fixes of 1, 2 refer to C1s and O1s spectra, respectively. Compared with FTIR spectra, XPS reveals more detailed information on the functional groups and chemical bonds.

3.2.2. Gel layer properties analyses

Fig. 7 shows the thermogravimetric analysis (TGA) results of different gels. It can be seen

that the TGA curve of these samples can be divided into two stages. When the temperature <100 ℃, the weights of all samples decreased sharply, which was ascribed to the evaporation of water. When the temperature rose above 200 ℃, a slight decrease of the weights was observed due to the evaporation of the alginate. Fig. 7 shows that there is difference in the thermal stability of alginate gel layers formed in three draw solutions with different ionic strength. According to reports, the thermal stability of alginate is affected by ions, which may be caused by the changes in the ability of gel layers to bind with water resulted from the cross-linking effect [58-60].

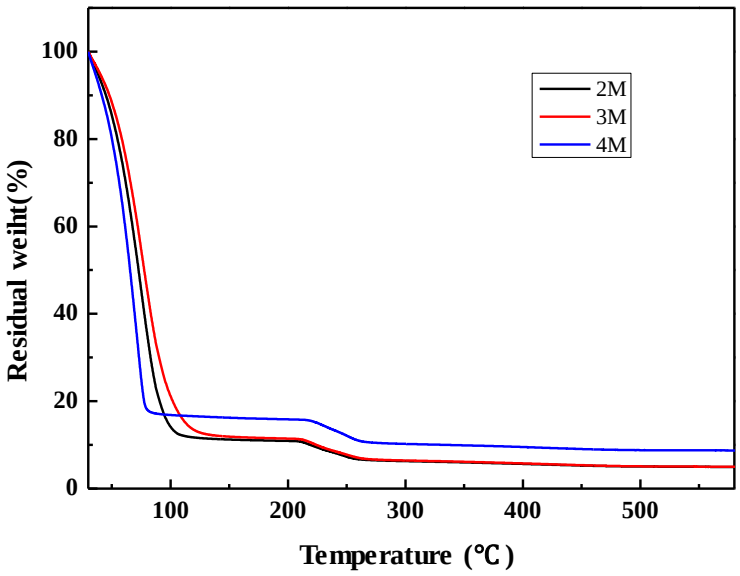

Fig. 7. TGA analysis of alginate gels formed in draw solutions with different ionic strength.

The ability of gel layers to bind with water can be verified by heating experiments [61]. The chemical potential of bound water in gel layers is much lower than that of free water, and this chemical potential gap needs to be overcome in order to drag the bound water in gel layers to the free water side [27]. Fig. 8 shows the amount of water loss in different gel layers under the same heating conditions, and the water loss decreased linearly with the NaCl content in gel layers. This result indicated that the bound water was more difficult to drag out from dense gel layers that contained a large amount of NaCl. In other words, considerable energy was

demanded in order to overcome the huge chemical potential gap to drag out bound water from dense gel layer with high NaCl content during the filtration, resulting in significant decline in FO membrane filtration efficiency [28]. Therefore, the effect of reverse diffusion of draw solution on the filtration behavior of alginate gel layer could be attributed to the ability of gel layer to bind with water. Previous studies reported that the ability of gel layer to bind with water was directly determined by the gel layer structure [27, 28, 62].

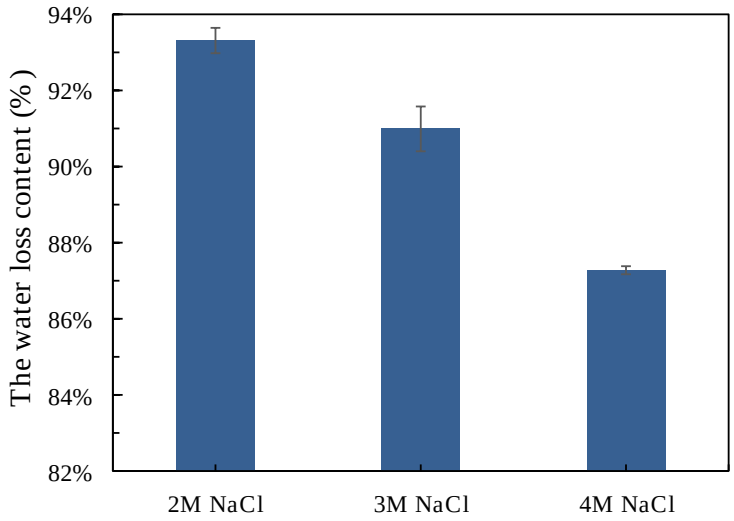

Fig. 8. Water loss of alginate gel layers formed in draw solutions with different ionic strength under heating conditions (heating time: 1 h, oven temperature: 35 ℃).

Fig. 9 presents the phase-contrast microscope images of molecular chain structures of fresh alginate gel layers formed in draw solutions with different ionic strength. To the best of our knowledge, this paper is the first direct microscopic observation study on the molecular chain structures of fresh fouling layers [8]. It is clear that the NaCl trapped in alginate gel layer had an appreciable effect on the arrangement of alginate chains in gel layer (Fig. 9). A lot of short alginate chains were sparsely distributed in alginate gel layer with low NaCl content (Fig. 9(a)), making the water in gel layer unable to be firmly bound. This was because short alginate chains moved away from each other due to the mutual exclusion of the polar carboxylic acid groups in alginate chains with low NaCl content [27, 28]. Short alginate chains cross-linked and produced

parallel and compact long alginate chains in Figs. 9(b) and (c), indicating that the large amount of NaCl trapped in alginate gel layers promoted the growth and symmetrical distribution of alginate chains. Long and dense alginate chains contributed to the formation of a compact molecular chain structure, which acted as the skeleton of gel layer and bound with the free water in feed solution to form a gel layer [47]. Hence, the results of Fig.8 and Fig.9 suggest that due to change of the molecular chain structure, the bound water is more difficult to drag out from the dense gel layer containing a large amount of NaCl. In view of this, fouling behavior of alginate solution in draw solution with different ionic strength (Figs. 2 and 3) could be reasonably attributed to the change in the structure of alginate chains in gel layer [38, 50, 63].

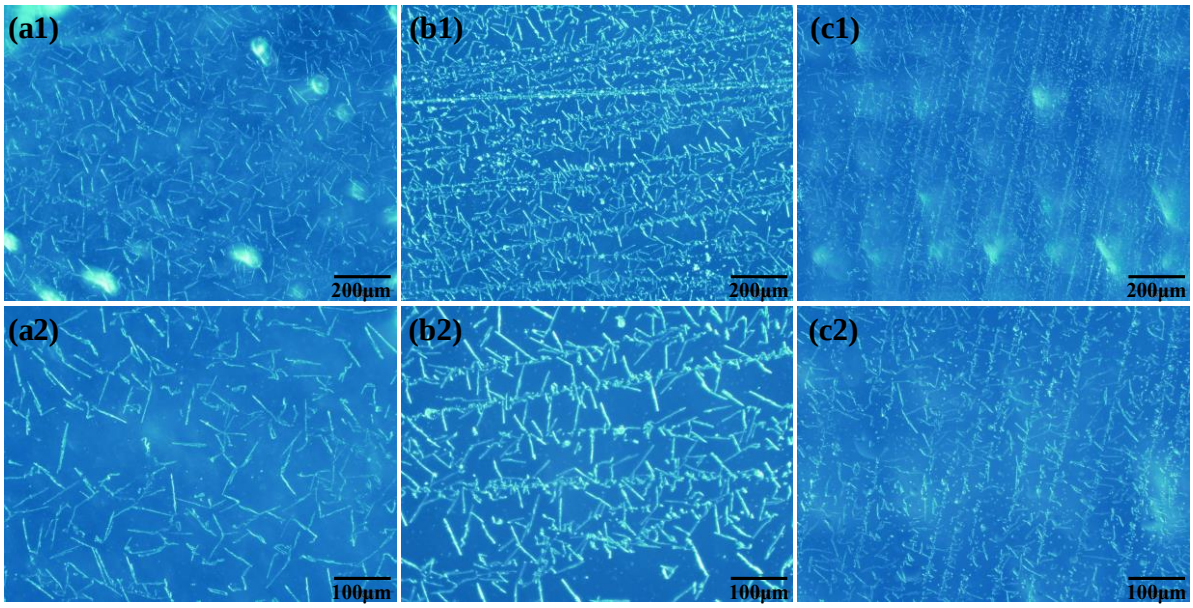

Fig. 9. Phase-contrast microscopy images of the molecular structure in alginate fouling layers formed in draw solutions with different ionic strength. (a) 2M, (b) 3M and (c) 4M NaCl solutions, and the 1, 2 represent 200 times and 400 magnifications, respectively.

Accordingly, exploring the forces that control this molecular structure transformation might provide essential fouling mechanisms for FO processes. In this paper, DFT analysis was used to simulate the interactions of alginate chains with varied content of NaCl. DFT simulation was performed to further determine the possible molecular structure changes (Fig. 9) of alginate gel

layers [46].

3.3. DFT simulation of alginate chains cross-linking behaviors

A computational model of two short alginate chains was constructed to explicate the intermolecular interaction [20, 47]. Fig. 10 shows that the energy of two alginate chains in vertical (-341.93 kcal/mol) and linear (-308.51 kcal/mol) states was very close and low, which illustrates when NaCl was absent in gel layers, the alginate chains can be arranged freely due to the mutual exclusion of the polar carboxylic acid groups in alginate chains. DFT simulation results could well explain the distribution of alginate chains in Fig. 9(a).

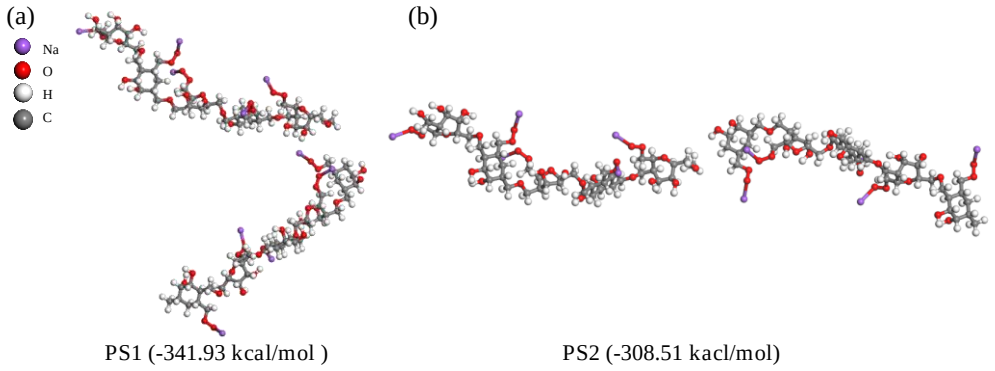

Fig. 10. Two optimized geometries for two single alginate chains that contained 10 uronic units but no NaCl.

Fig. 11 shows the states between two long alginate chains at low and high NaCl content. DFT calculations revealed the relative low energy of two parallel long alginate chains, indicating that the parallel state was energetically stable. The reason was that when NaCl present, the intermolecular interactions of two hydrogen bonds formed by the hydroxyl and carboxyl groups of the aldaldehyde rings at terminals of alginate chains ensured the aldaldehyde rings tightly connected but parallel to each other [47]. At low NaCl content, the distance between the two hydrogen bonds of two alginate chains was 3.06 Å and the energy was -20.87 kcal/mol (Fig. 11(a)). However, the distance between the two alginate chains was 2.18 Å, with lower energy

(-104.79 kcal/mol) at high ionic strength (Fig. 11(b)). To summarize, the simulation results demonstrated that the NaCl trapped in gel layers could shorten the distance between hydrogen bonds and lower the energy of alginate chain terminals.

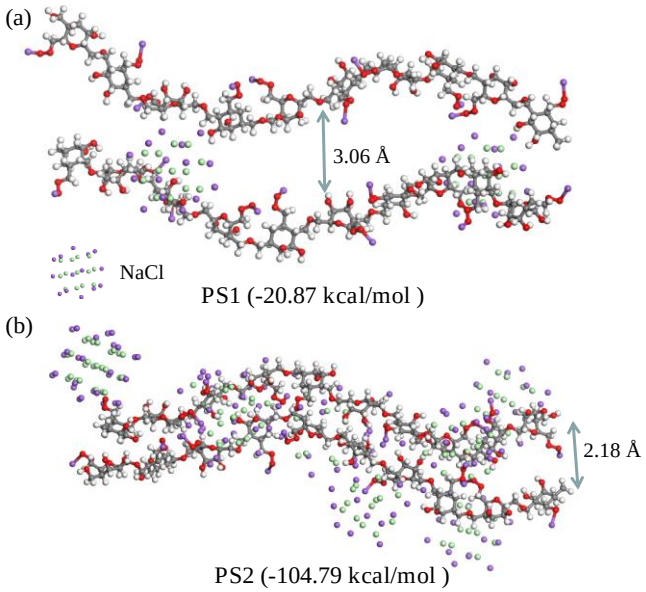

Fig. 11. Two optimized geometries of long alginate chains containing 20 uronic units: (a) low NaCl content and (b) high NaCl content.

Figs. 10 and 11 provide structural and energy information of alginate molecular chains with varied content of NaCl. It is clear that alginate chains were mutually repulsive at extremely low NaCl content or in the absence of NaCl, while the presence of NaCl ensured that the terminal aldehyde-aldehyde rings were tightly connected and parallel to each other due to the hydrogen bonds existing between the carboxyl groups at the terminals of alginate chains [28]. As the NaCl content in gel layer increased, the distance and the energy between hydrogen bonds formed by two carboxyl groups decreased. Consequently, two long alginate chains stayed in closer proximity to each other and thus formed a regular and dense alginate layer. According to the formation mechanism of alginate chain structures with varied content of NaCl revealed by DFT simulation, the reverse diffusion of draw solutions or the ion content in gel layers had a critical

influence on the molecular chain structure and interaction of alginate gel layers (Fig. 9). According to the formation mechanism of alginate chain structures with varied NaCl content revealed by DFT simulation, the reverse diffusion of draw solutions or the ion content in gel layers had a critical influence on the molecular chain structure and interaction of alginate gel layer (Fig. 9).

3.4. Mechanistic insights into FO membrane fouling behaviors

The above-mentioned advanced techniques including phase-contrast microscope and DFT simulation provided detailed structure information of alginate gel layers formed in draw solutions with different ionic strength. Based on these results, Fig. 12 introduces a schematic diagram of the effect mechanisms of reverse diffusion of draw solution on the fouling behavior of alginate layer.

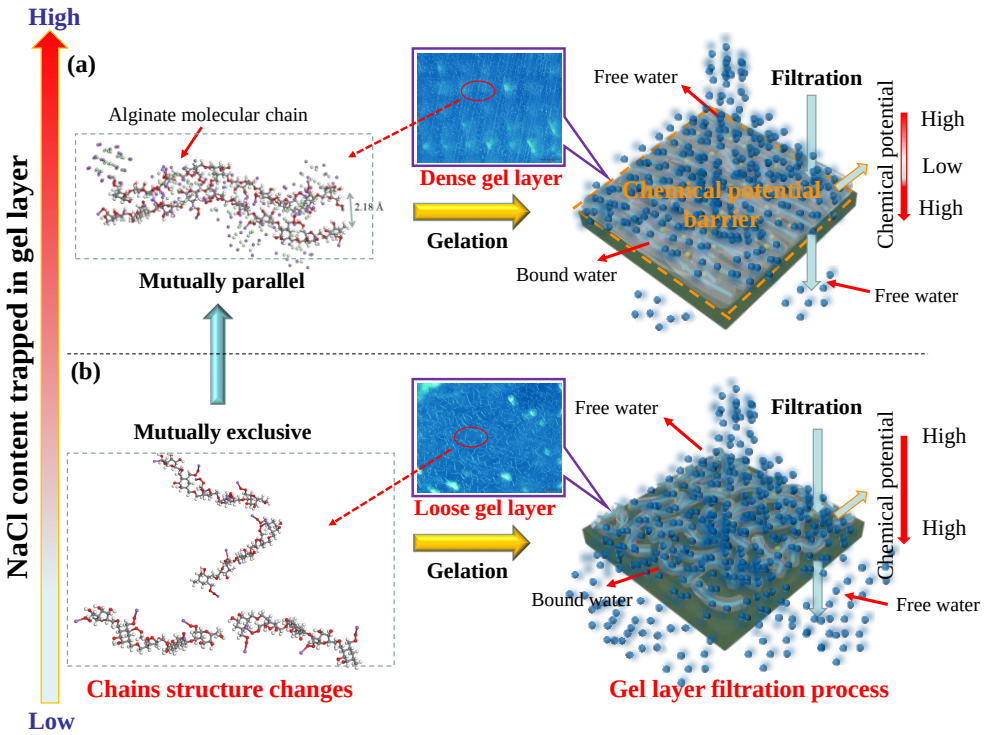

Fig. 12. Schematic diagram of the cross-linking process of alginate chains affected by reverse NaCl and the filtration process of alginate layers governed by Flory-Huggins mechanism.

It can be seen from Fig.12(b) that the gel layers (shown in Figs. 3(b1) and (b2)) formed on the FO membrane surface were very loose at low content of reverse diffused NaCl due to the repulsion between carboxylic acid groups on the alginate chains. These loose gel structures could not effectively bind with water, so making it impossible to substantially lower the water flux (Figs. 2(a) and (b)) [25, 64]. However, a large amount of NaCl trapped in gel layers reduced the repulsion between the alginate chains and shortened the distance between hydrogen bonds at the two terminals of alginate chains, thereby providing a highly cross-linked polymeric network (Fig. 12(a)) [28]. According to the Flory-Huggins lattice theory expressed by Eq. (5), the chemical potential change accompany by the formation of gel layer is dependent on polymerization degree, and highly cross-linked network corresponds to higher chemical potential change. From thermodynamic viewpoint, filtration through a gel layer can be regarded as the inverse process of gel formation. Therefore, filtration through a denser gel layer (Fig. 12(a)) is considered as dragging water from gel layer (much low chemical potential) to permeate side (high chemical potential) [24, 65]. In other words, dense gel layer functioned as a "chemical potential barrier", which offset a part of chemical potential gap between draw solution and feed solution, resulting in water penetration becomes difficult. During the FO membrane filtration process of gel, the osmotic pressure gap ($\Delta\pi_{gel}$) was used to overcome the water chemical potential gap ($\Delta\mu_{gel}$) between draw solution and gel layer [17]:

$$\Delta\mu_{gel} = -V_B\Delta\pi_{gel} \quad (6)$$

where V_B represents the molar volume of solvent and is generally considered to be equal to the molar volume of the dilute solution (V), $\Delta\pi_{gel}$ is the part of osmotic pressure gap ($\Delta\pi_{drive}$) that is used to overcome the chemical potential gap between gel layer and combination of free water and pure polymers ($\Delta\mu_{gel}$). Substituting Eq. (5) into Eq. (6), According to Flory-Huggins theory,

$\Delta\pi_{gel}$ can be calculated by:

$$\Delta\pi_{gel} = -\Delta\mu_{gel} / V_B = -RT\left[\ln\left(1-\phi_2\right)+\left(1-N^{-1}\right)\phi_2+\chi\phi_2^2\right]/V_B \quad (7)$$

For FO membrane filtration processes, the trapped NaCl in gel layer also contributes osmotic pressure (π_{NaCl}), which can be calculated by Eq. 2. Therefore, during gel layer filtration, the net osmotic pressure gap ($\Delta\pi_{net}$) can be described by:

$$\Delta\pi_{net} = \Delta\pi_{drive} - \Delta\pi_{gel} - \pi_{NaCl} \quad (8)$$

The above Eqs were perfect for the description of the chemical potential since previous studies have calculated the chemical potential of agar gels and based on these Eqs [17, 19]. The calculation results suggested that the chemical potential gap between gel layer and permeate was huge, so the $\Delta\pi_{gel}$ used to overcome this chemical potential gap may be extremely high [17, 61]. $\Delta\pi_{gel}$ can be quantitatively assessed by Eq. (7) provided that several thermodynamic parameters are determined. Due to the χ value of alginate has not been reported and is difficult to be estimated, it is hard to conduct quantitative simulation of variation of the Flory-Huggins induced chemical potential gap with the degree of polymerization [27]. The degree of polymerization of the polymer chains increased with the rising content of NaCl. Although it is hard to conduct a quantitative simulation of the variation of the Flory-Huggins induced the $\Delta\mu_{gel}$ with the degree of polymerization. The general profile of relation between Flory-Huggins induced the $\Delta\mu_{gel}$ and polymerization degree could be depicted by Eq. (5). According to Eq. (5) and Eq. (7), $\Delta\mu_{gel}$ decrease with the degree of polymerization, which corresponded to $\Delta\pi_{gel}$ increase, resulting in more flux decline. The real existence of the $\Delta\pi_{gel}$ induced by Flory-Huggins mechanism was confirmed by quantifying the changes in osmotic pressure during FO membrane filtration.

In the filtration experiment of alginate solutions in 4 mol/L NaCl draw solution ($\Delta\pi_{drive}$ is

24662.16 kPa). After filtration of 500 mL foulants, the $\Delta\pi_{drive}$ was diluted to 22705.49 kPa, as can be calculated by converting the conductivity gap between draw solution and feed solution, and its driving force decreased by 7.9% compared with that in the initial stage. However, water flux decreased by about 69.2%, suggesting that the $\Delta\pi_{net}$ at this time was only 7595.95 kPa (30.8%×24662.16 kPa). This meant that the osmotic pressure gap offset by gel layer should be 15109.54 kPa (22705.49 kPa-7595.95 kPa). It is important to note that the osmotic pressure of the gel layer includes the π_{NaCl} caused by reverse diffused NaCl and the $\Delta\pi_{gel}$. The concentration of NaCl trapped in the gel layer was then measured to be 0.60 mol/L by the inductively coupled plasma, and the π_{NaCl} was 2780.67 kPa. Thus, the $\Delta\pi_{gel}$ to overcome the chemical potential gap of this gel layer was calculated to be 12328.87 kPa (15109.54 kPa-2780.67 kPa) by Eq. (8), accounting for 54.30% of the $\Delta\pi_{drive}$ of 4 mol/L NaCl draw solution. Seen from the calculation results, the osmotic pressure gap required to overcome the chemical potential gap between gel layer and draw solution was extremely high, which offsets a lot of driving force. Filtration experiments show that the $\Delta\pi_{gel}$ increased with the degree of polymerization of the polymer chains rising, resulting in decrease of the net osmotic pressure gap, corresponding to flux decrease. The increase trend of the $\Delta\pi_{gel}$ depicted by Eq. (7) was consistent with filtration experiment results. Therefore, the Flory-Huggins theory not only provided a description of mechanism of chemical potential gap during the FO filtration process, but also explained the fouling tendency of alginate solution with reverse diffusion of solution.

4. Conclusions

Filtration tests showed that the reverse diffusion of draw solutions had critical effects on FOMBR filtration behavior of alginate solutions. Phase-contrast microscope images and DFT calculation results proved at the molecular level that the content of ions trapped in gel layers

directly determined the molecular chain structure of gel layers. Moreover, heating experiments confirmed that gel layers with high NaCl content required more energy to drag out bound water, indicating that gel layer acted as a "chemical potential barrier" that prevented bound water from turning into free water. The above results established for the first time that the gel layer (the "chemical potential barrier") was primarily affected by changes of the layer's molecular chain structure. Subsequently, the "chemical potential barrier" described by Flory-Huggins theory was proposed to elucidate the FOMBR fouling behavior affected by reverse diffusion of draw solutions from the perspective of chemical potential changes. This hand-in-hand method of combining experimental characterizations and theoretical calculations provided a comprehensive understanding of the effect of reverse diffusion of draw solution on alginate fouling properties.

Acknowledgments

This work was financially supported by China National Key Project of Science and Technology "Major Science and Technology Program for Water Pollution Control and Treatment" (2018ZX07601001).

Reference

[1] C.W. King, M.E. Webber, Water Intensity of Transportation, Environ. Sci. Technol., 42 (2008) 7866-7872.

[2] F. Meng, S. Zhang, Y. Oh, Z. Zhou, H.-S. Shin, S.-R. Chae, Fouling in membrane bioreactors: An updated review, Water Res., 114 (2017) 151-180.

[3] M.A. Shannon, P.W. Bohn, M. Elimelech, J.G. Georgiadis, B.J. Mariñas, A.M. Mayes, Science and technology for water purification in the coming decades, Nature, (2008).

[4] A. Achilli, T.Y. Cath, E.A. Marchand, A.E. Childress, The forward osmosis membrane bioreactor: A low fouling alternative to MBR processes, Desalination, 239 (2009) 10-21.

[5] S. Zhao, L. Zou, C.Y. Tang, D. Mulcahy, Recent developments in forward osmosis: Opportunities and challenges, J. Membr. Sci., 396 (2012) 1-21.

[6] X. Wang, V.W.C. Chang, C.Y. Tang, Osmotic membrane bioreactor (OMBR) technology for wastewater treatment and reclamation: Advances, challenges, and prospects for the future, J. Membr. Sci., 504 (2016) 113-132.

[7] P. Nasr, H. Sewilam, Forward osmosis: an alternative sustainable technology and potential applications in water industry, Clean Technologies and Environmental Policy, 17 (2015) 2079-2090.

[8] Y. Wang, F. Wicaksana, C.Y. Tang, A.G. Fane, Direct Microscopic Observation of Forward Osmosis Membrane Fouling, Environ. Sci. Technol., 44 (2010) 7102-7109.

[9] H. Zhang, Y. Ma, T. Jiang, G. Zhang, F. Yang, Influence of activated sludge properties on flux behavior in osmosis membrane bioreactor (OMBR), J. Membr. Sci., 390-391 (2012) 270-276.

[10] E.R. Cornelissen, D. Harmsen, K.F. de Korte, C.J. Ruiken, J.-J. Qin, H. Oo, L.P. Wessels, Membrane fouling and process performance of forward osmosis membranes on activated sludge, J. Membr. Sci., 319 (2008) 158-168.

[11] C. Boo, S. Lee, M. Elimelech, Z. Meng, S. Hong, Colloidal fouling in forward osmosis: Role of reverse salt diffusion, J. Membr. Sci., 390-391 (2012) 277-284.

[12] Q. She, R. Wang, A.G. Fane, C.Y. Tang, Membrane fouling in osmotically driven membrane processes: A review, J. Membr. Sci., 499 (2016) 201-233.

[13] S. Zou, Y. Gu, D. Xiao, C.Y. Tang, The role of physical and chemical parameters on

491 forward osmosis membrane fouling during algae separation, J. Membr. Sci., 366 (2011)
492 356-362.
493 [14] J.S. Yong, W.A. Phillip, M. Elimelech, Coupled reverse draw solute permeation and
494 water flux in forward osmosis with neutral draw solutes, J. Membr. Sci., 392-393 (2012) 9-17.
495 [15] W.A. Phillip, J.S. Yong, M. Elimelech, Reverse Draw Solute Permeation in Forward
496 Osmosis: Modeling and Experiments, Environ. Sci. Technol., 44 (2010) 5170-5176.
497 [16] X.-M. Wang, T.D. Waite, Impact of gel layer formation on colloid retention in
498 membrane filtration processes, J. Membr. Sci., 325 (2008) 486-494.
499 [17] J. Chen, M. Zhang, F. Li, L. Qian, H. Lin, L. Yang, X. Wu, X. Zhou, Y. He, B.-Q. Liao,
500 Membrane fouling in a membrane bioreactor: High filtration resistance of gel layer and its
501 underlying mechanism, Water Res., 102 (2016) 82-89.
502 [18] X.-m. Wang, T.D. Waite, Role of Gelling Soluble and Colloidal Microbial Products in
503 Membrane Fouling, Environ. Sci. Technol., 43 (2009) 9341-9347.
504 [19] J. Teng, L. Shen, G. Yu, F. Wang, F. Li, X. Zhou, Y. He, H. Lin, Mechanism analyses
505 of high specific filtration resistance of gel and roles of gel elasticity related with membrane
506 fouling in a membrane bioreactor, Bioresour. Technol., 257 (2018).
507 [20] J. Teng, Y. Chen, G. Ma, H. Hong, T. Sun, B.-Q. Liao, H. Lin, Membrane fouling by
508 alginate in polyaluminum chloride (PACl) coagulation/microfiltration process: Molecular
509 insights, Sep. Purif. Technol., 236 (2020) 116294.
510 [21] H. Hong, M. Zhang, Y. He, J. Chen, H. Lin, Fouling mechanisms of gel layer in a
511 submerged membrane bioreactor, Bioresour. Technol., 166 (2014) 295-302.
512 [22] H. Lin, M. Zhang, F. Wang, F. Meng, B.-Q. Liao, H. Hong, J. Chen, W. Gao, A critical
513 review of extracellular polymeric substances (EPSs) in membrane bioreactors: Characteristics,

514 roles in membrane fouling and control strategies, J. Membr. Sci., 460 (2014) 110-125.
515 [23] R. Bai, H.F. Leow, Microfiltration of activated sludge wastewater—the effect of
516 system operation parameters, Sep. Purif. Technol., 29 (2002) 189-198.
517 [24] T. Sakai, J.-i. Horinaka, T. Takigawa, A new method to estimate the sol–gel transition
518 entropy in physically gelling systems, Polymer Journal, 47 (2014) 244-248.
519 [25] Q. Lei, M. Zhang, L. Shen, R. Li, B.-Q. Liao, H. Lin, A novel insight into membrane
520 fouling mechanism regarding gel layer filtration: Flory-Huggins based filtration mechanism,
521 SCI. Rep., 6 (2016) 33343.
522 [26] W. Mönch, J. Dehnert, E. Jaufmann, H. Zappe, Flory-Huggins swelling of polymer
523 Bragg mirrors, Applied Physics Letters, 89 (2006) 164104-164104.
524 [27] M. Zhang, H. Hong, H. Lin, L. Shen, H. Yu, G. Ma, J. Chen, B.Q. Liao, Mechanistic
525 insights into alginate fouling caused by calcium ions based on terahertz time-domain spectra
526 analyses and DFT calculations, Water Res., 129 (2017) 337-346.
527 [28] X. You, J. Teng, Y. Chen, Y. Long, G. Yu, L. Shen, H. Lin, New insights into
528 membrane fouling by alginate: Impacts of ionic strength in presence of calcium ions,
529 Chemosphere, 246 (2020) 125801.
530 [29] G. Singh, L. Song, Quantifying the effect of ionic strength on colloidal fouling
531 potential in membrane filtration, J. Colloid Interf. Sci., 284 (2005) 630-638.
532 [30] S. Bhattacharjee, M. Elimelech, Surface Element Integration: A Novel Technique for
533 Evaluation of DLVO Interaction between a Particle and a Flat Plate, J. Colloid Interf. Sci., 193
534 (1997) 273-285.
535 [31] J. Teng, L. Shen, Y. He, B.Q. Liao, G. Wu, H. Lin, Novel insights into membrane
536 fouling in a membrane bioreactor: Elucidating interfacial interactions with real membrane

surface, Chemosphere, 210 (2018) 769.

[32] S. Bhattacharjee, C.-H. Ko, M. Elimelech, DLVO Interaction between Rough Surfaces, Langmuir, 14 (1998).

[33] B. Mi, M. Elimelech, Organic fouling of forward osmosis membranes: Fouling reversibility and cleaning without chemical reagents, J. Membr. Sci., 348 (2010) 337-345.

[34] S. Meng, Y. Liu, Alginate block fractions and their effects on membrane fouling, Water Res., 47 (2013) 6618-6627.

[35] M. Herzberg, M. Elimelech, Biofouling of reverse osmosis membranes: Role of biofilm-enhanced osmotic pressure, J. Membr. Sci., 295 (2007) 11-20.

[36] M. Herzberg, S. Kang, M. Elimelech, Role of Extracellular Polymeric Substances (EPS) in Biofouling of Reverse Osmosis Membranes, Environ. Sci. Technol., 43 (2009) 4393-4398.

[37] J. Ji, J. Qiu, F.-s. Wong, Y. Li, Enhancement of filterability in MBR achieved by improvement of supernatant and floc characteristics via filter aids addition, Water Res., 42 (2008) 3611-3622.

[38] J. Teng, M. Zhang, K.-T. Leung, J. Chen, H. Hong, H. Lin, B.-Q. Liao, A unified thermodynamic mechanism underlying fouling behaviors of soluble microbial products (SMPs) in a membrane bioreactor, Water Res., 149 (2019) 477-487.

[39] H.J. Lin, K. Xie, B. Mahendran, D.M. Bagley, K.T. Leung, S.N. Liss, B.Q. Liao, Sludge properties and their effects on membrane fouling in submerged anaerobic membrane bioreactors (SAnMBRs), Water Res., 43 (2009) 3827-3837.

[40] C.Y. Tang, T.H. Chong, A.G. Fane, Colloidal interactions and fouling of NF and RO membranes: A review, Adv. Colloid Interf. Sci., 164 (2011) 126-143.

[41] H.T. Nguyen, N.C. Nguyen, S.-S. Chen, H.H. Ngo, W. Guo, C.-W. Li, A new class of draw solutions for minimizing reverse salt flux to improve forward osmosis desalination, Science of The Total Environment, 538 (2015) 129-136.

[42] M. Park, J.H. Kim, Numerical analysis of spacer impacts on forward osmosis membrane process using concentration polarization index, J. Membr. Sci., 427 (2013) 10-20.

[43] Z. Wang, Z. Wu, X. Yin, L. Tian, Membrane fouling in a submerged membrane bioreactor (MBR) under sub-critical flux operation: Membrane foulant and gel layer characterization, J. Membr. Sci., 325 (2008) 238-244.

[44] G.E. Palade, Studies on the Endoplasmic Reticulum: II. Simple Dispositions in Cells in Situ, The Journal of Biophysical and Biochemical Cytology, 1 (1955) 567-582.

[45] Y.-X. Yu, A dispersion-corrected DFT study on adsorption of battery active materials anthraquinone and its derivatives on monolayer graphene and h-BN, Journal of Materials Chemistry A: Materials for Energy and Sustainability, 2 (2014) 8910-8917.

[46] M. Shkir, S. Muhammad, S. AlFaify, Experimental and density functional theory (DFT): A dual approach to study the various important properties of monohydrated l-proline cadmium chloride for nonlinear optical applications, Spectrochim. Acta A, 143 (2015) 128-135.

[47] M. Zhang, H. Hong, H. Lin, L. Shen, H. Yu, G. Ma, J. Chen, B.-Q. Liao, Mechanistic insights into alginate fouling caused by calcium ions based on terahertz time-domain spectra analyses and DFT calculations, Water Res., 129 (2018) 337-346.

[48] P.J. Flory, Thermodynamics of High Polymer Solutions, J. Chem. Phys., 9 (1941) 660.

[49] M. L. Huggins, Thermodynamic Properties of Solutions of Long Chain Compounds, 2006.

[50] Y. Long, X. You, Y. Chen, H. Hong, B.-Q. Liao, H. Lin, Filtration behaviors and

583 fouling mechanisms of ultrafiltration process with polyacrylamide flocculation for water
584 treatment, Science of The Total Environment, 703 (2020) 135540.
585 [51] P.J. Flory, Molecular theory of rubber elasticity, Polymer, 20 (1979) 1317-1320.
586 [52] B. Mi, M. Elimelech, Chemical and physical aspects of organic fouling of forward
587 osmosis membranes, J. Membr. Sci., 320 (2008) 292-302.
588 [53] X. Song, M. Xie, Y. Li, G. Li, W. Luo, Salinity build-up in osmotic membrane
589 bioreactors: Causes, impacts, and potential cures, Bioresour. Technol., 257 (2018).
590 [54] D. Xiao, C.Y. Tang, J. Zhang, W.C.L. Lay, R. Wang, A.G. Fane, Modeling salt
591 accumulation in osmotic membrane bioreactors: Implications for FO membrane selection and
592 system operation, J. Membr. Sci., 366 (2011) 314-324.
593 [55] M.G. Sankalia, R.C. Mashru, J.M. Sankalia, V.B. Sutariya, Reversed chitosan–alginate
594 polyelectrolyte complex for stability improvement of alpha-amylase: Optimization and
595 physicochemical characterization, European Journal of Pharmaceutics and Biopharmaceutics, 65
596 (2007) 215-232.
597 [56] Z.-H. Hu, A.M. Omer, X.k. Ouyang, D. Yu, Fabrication of carboxylated cellulose
598 nanocrystal/sodium alginate hydrogel beads for adsorption of Pb(II) from aqueous solution, Int.
599 J. Biol. Macromol., 108 (2018) 149-157.
600 [57] K. Kimura, T. Kakuda, H. Iwasaki, Membrane fouling caused by lipopolysaccharides:
601 A suggestion for alternative model polysaccharides for MBR fouling research, Sep. Purif.
602 Technol., 223 (2019) 224-233.
603 [58] Y. Pan, W. Wang, L. Liu, H. Ge, L. Song, Y. Hu, Influences of metal ions crosslinked
604 alginate based coatings on thermal stability and fire resistance of cotton fabrics, Carbohyd.
605 Polym., 170 (2017) 133-139.

606 [59] Y. Liu, J.-S. Wang, P. Zhu, J.-C. Zhao, C.-J. Zhang, Y. Guo, L. Cui, Thermal
607 degradation properties of biobased iron alginate film, J. Anal. Appl. Pyrol., 119 (2016) 87-96.
608 [60] Q. Lei, F. Li, L. Shen, L. Yang, B.-Q. Liao, H. Lin, Tuning anti-adhesion ability of
609 membrane for a membrane bioreactor by thermodynamic analysis, Bioresour. Technol., 216
610 (2016) 691-698.
611 [61] Q. Lei, M. Zhang, L. Shen, R. Li, B.Q. Liao, H. Lin, A novel insight into membrane
612 fouling mechanism regarding gel layer filtration: Flory-Huggins based filtration mechanism,
613 SCI. Rep., 6 (2016) 33343.
614 [62] Y. Chen, J. Teng, B.-Q. Liao, R. Li, H. Lin, Molecular insights into the impacts of
615 iron(III) ions on membrane fouling by alginate, Chemosphere, 242 (2020) 125232.
616 [63] Y. Chen, L. Shen, R. Li, X. Xu, H. Hong, H. Lin, J. Chen, Quantification of interfacial
617 energies associated with membrane fouling in a membrane bioreactor by using BP and GRNN
618 artificial neural networks, J. Colloid Interf. Sci., 565 (2020) 1-10.
619 [64] W. Borchard, U. Steinbrecht, Theory of swelling of a crosslinked substance in
620 equilibrium with a solvent in various phases, Colloid & Polymer Science, 269 (1991) 95-104.
621 [65] J. Teng, M. Wu, J. Chen, H. Lin, Y. He, Different fouling propensities of loosely and
622 tightly bound extracellular polymeric substances (EPSs) and the related fouling mechanisms in a
623 membrane bioreactor, Chemosphere, 255 (2020) 126953.
624

Conflict of Interest

The authors declared that they have no conflicts of interest to this work.

We declare that we do not have any commercial or associative interest that represents a conflict of interest in connection with the work submitted.

Author Statement

Jiaheng Teng: Investigation, Methodology, Writing - original draft.

Hanmin Zhang: Conceptualization, Funding acquisition, Project administration, Writing - review & editing.

Chuyang Tang: Investigation, Data curation, Formal analysis.

Hongjun Lin: Investigation, Data curation, Formal analysis.